Composites Science and Technology 79 (2013) 15–20

Contents lists available at SciVerse ScienceDirect

Composites Science and Technology

journal homepage: www.elsevier.com/locate/compscitech

Self-sealing of mechanical damage in a fully cured structural composite

Jericho L. Moll [a], Henghua Jin [b,c], Chris L. Mangun [d], Scott R. White [b,c], Nancy R. Sottos [a,b,*]

[a] Department of Materials Science and Engineering, University of Illinois at Urbana-Champaign, Urbana, IL 61801, USA
[b] Beckman Institute for Advanced Science and Technology, University of Illinois at Urbana-Champaign, Urbana, IL 61801, USA
[c] Department of Aerospace Engineering, University of Illinois at Urbana-Champaign, Urbana, IL 61801, USA
[d] CU Aerospace, Champaign, IL 61820, USA

ARTICLE INFO

Article history:
Received 27 August 2012
Received in revised form 9 January 2013
Accepted 6 February 2013
Available online 16 February 2013

Keywords:
Self-healing
Woven composite
Microcrack
Autonomic
Microcapsules

ABSTRACT

A two part healing chemistry, stable to 150 °C, is incorporated in a woven glass/epoxy fiber-reinforced composite with a glass transition temperature (T_g) of 127 °C. The healing system is comprised of one type of microcapsules containing silanol end-functionalized polydimethylsiloxane, and a crosslinking agent, polydiethoxysilane, and a second type containing dibutyltin dilaurate catalyst in the solvent hexylacetate. The effects of microcapsule size and concentration on self-healing and mechanical properties including short beam strength, storage modulus and T_g were investigated. Self-healing of mechanical damage is assessed through the use of a pressure cell apparatus to detect nitrogen flow through a damaged composite. Complete self-healing was achieved when 42 μm diameter microcapsules at a loading of 9 vol.% or 25 μm microcapsules at a loading of 11 vol.% were added to the matrix.

1. Introduction

Microcracking in advanced composites leads to a reduction in stiffness and an increase in permeability. In cryogenic tanks, microcracks form during thermal cycling due to the coefficient of thermal expansion mismatch between the fibers and the matrix. When a sufficient density of microcracks form a percolating network through the thickness of the composite, cryogens begin to leak through the tank wall [1]. In sandwich structures, mechanical fatigue or low velocity impact can also induce microcracking and an increase in water absorption into the core material, which not only increases the overall weight of the composite, but can also cause delaminations between the face sheet and core [2].

Stacking sequence and fiber architecture affect the permeability of composites during and after thermal cycling due to the development of thermal stresses in the plies [3,4]. In an effort to minimize leakage caused by cryogenic cycling and low velocity impacts, McVay et al. embedded flexible barrier layers within a composite and demonstrated a 290% improvement over composites without the barrier layers [5]. Beiermann et al. introduced encapsulated polydimethylsiloxane (PDMS) based healing components into the PDMS layer of a polyurethane/nylon/PDMS laminate [6]. Damage induced a polycondensation reaction between the encapsulated healing components effectively filling the puncture and regaining the ability to seal. Kalista et al. reported a self-healing poly(ethylene-co-methacrylic acid) copolymer capable of autonomic molecular rearrangement which was able to maintain pressure up to 3 MPa after projectile puncture damage [7]. Self-healing in this ionomer was attributed to a two-step melt elastic recovery and inter-chain diffusion self-healing mechanism. Moll et al. demonstrated the ability to self-heal 67% of samples and prevent gas phase leakage across a mechanically damaged woven composite containing microencapsulated dicyclopentadiene (DCPD) and wax protected Grubbs' catalyst [8]. Due to limitations in thermal stability of the healing chemistry, these composites could not be processed at elevated temperatures and the resulting glass transition temperature was approximately 60 °C.

Here we present a thermally stable microencapsulated self-healing chemistry which has previously been used as a healing agent in epoxy and bulk PDMS [9–11]. Both types of microcapsules in this dual capsule healing system are dispersed in the epoxy matrix. Crack damage ruptures the capsules releasing healing agents into the crack plane. Once the healing agents mix by diffusion, polymerization in the crack plane bonds the crack faces together, effectively healing the matrix. In our system, the first type of microcapsule contains a low viscosity PDMS oligomer and cross-linker while the second type contains a tin catalyst. These components are incorporated in the epoxy matrix of a woven composite, which is cured at an elevated temperature of 121 °C. Self-healing ability is evaluated for a range of capsules sizes and concentrations and their effect on mechanical properties is investigated.

* Corresponding author. Address: 1304 W. Green St., Urbana, IL 61801, United States. Tel.: +1 217 244 6901.
E-mail address: n-sottos@illinois.edu (N.R. Sottos).

0266-3538/$ - see front matter © 2013 Elsevier Ltd. All rights reserved.
http://dx.doi.org/10.1016/j.compscitech.2013.02.006

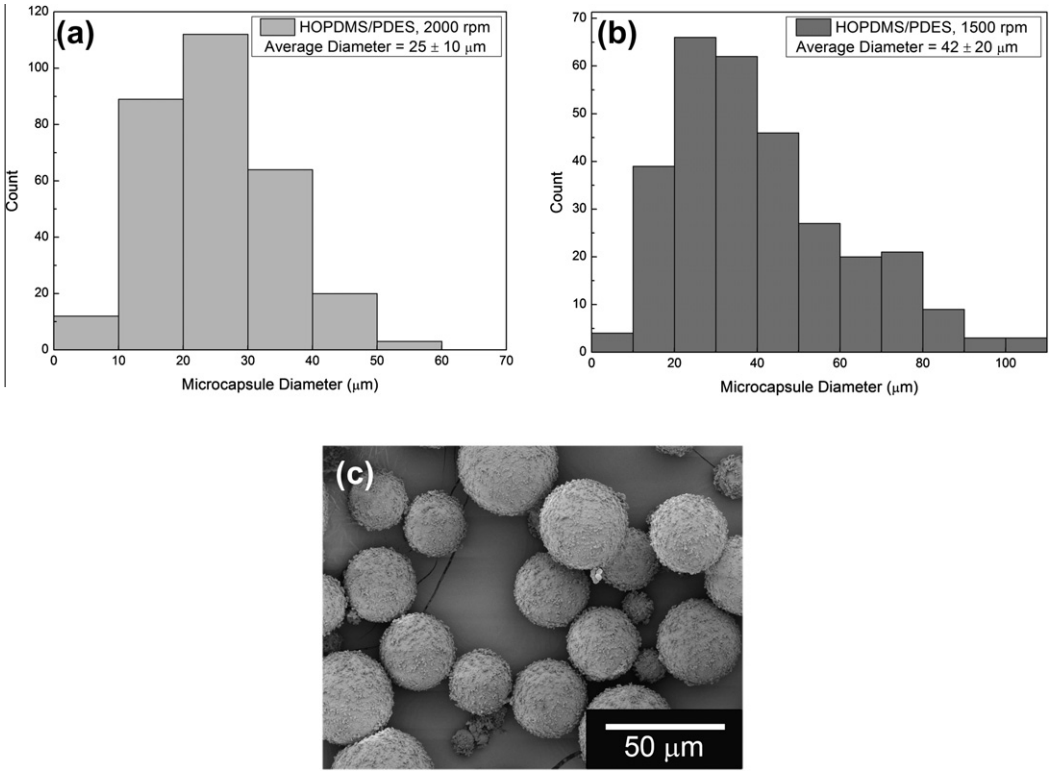

Fig. 1. Summary of HOPDMS/PDES microcapsules used in the healing portion of this study: (a) capsules prepared at an agitation rate of 2000 rpm with a number average diameter of 25 μm, (b) capsules prepared at an agitation rate of 1500 rpm with a number average diameter of 42 μm, (c) scanning electron microscope image of 25 μm capsules.

2. Materials and methods

2.1. Microencapsulated healing agent preparation

A PDMS healing agent and a catalyst were successfully encapsulated in two separate types of microcapsules. The first type of microcapsule was comprised of a mixture of 53 wt.% hydroxyl end-functionalized polydimethylsiloxane (HOPDMS) with the balance polydiethoxysiloxane (PDES) encapsulated in a urea–formaldehyde shell (both obtained from Gelest). The second type of microcapsule contained a 50:50 (by weight) mixture of dibutyltin dilaurate (DBTL) catalyst from Gelest and hexylacetate from Sigma Aldrich, which acts as a carrier solvent, encapsulated in a polyurethane shell.

The microcapsules containing HOPDMS and PDES were produced using an emulsion *in situ* polymerization exactly as described previously [6,9,10] for S21 HOPDMS. Microcapsules for self-healing with a urea formaldehyde shell wall and average diameters of 25 ± 10 μm (2000 rpm) and 42 ± 20 μm (1500 rpm) were produced by varying the agitation rate. Representative histograms for each agitation rate and a scanning electron microscope image of HOPDMS/PDES microcapsules manufactured at 2000 rpm (25 ± 10 μm) are presented in Fig. 1.

The microcapsules containing either pure hexylacetate or a 50:50 mixture of hexylacetate and DBTL (Fig. 2c) were manufactured using an oil in water emulsion interfacial polymerization similar to the one described by Mangun et al. [9] with the following notable exceptions. In a 600 mL beaker 2.5 g gum arabic (Sigma–Aldrich) was dissolved in 100 mL of deionized water under agitation at 1100 rpm. In a separate container 17 g hexylacetate or 10 g hexylacetate and 10 g DBTL were combined along with 2.5 g Desmodur L75 polyurethane prepolymer (Bayer) and added to the gum arabic solution at 85 °C. This solution was mixed for 1 h before the agitation rate was decreased to 200 rpm and the temperature was adjusted to room temperature for 1 h. Next, 50 mL of deionized water and 25 mL of 2.5 wt.% ethylene maleic anhydride solution (Zeeland Chemical) were added to the mixture while the agitation rate was kept constant and the temperature was adjusted to 55 °C for 4 h. Excess surfactant was eliminated from the aqueous capsule solution by centrifuging four times for 30 min at 1000 rpm, discarding the supernatant and replacing with deionized water after each centrifugation cycle. Finally, the solution was either frozen in liquid nitrogen and placed on a freeze drier to sublime off the water or filtered and allowed to air dry into free flowing microcapsules (Fig. 2c). Microcapsules with a polyurethane shell wall were produced with 20–40 μm average diameters. Representative histograms of size distributions for both DBTL/hexylacetate and pure hexylacetate microcapsules used in the healing portion of this study are provided in Fig. 2a and b.

2.2. Sample types

Three types of samples were fabricated for the healing portion of this study with the components of each summarized in Table 1. Control 1 samples were comprised of epoxy resin and E-glass reinforcement (no microcapsules). Control 2 samples contained not only the epoxy resin and E-glass reinforcement, but also HOPDMS/PDES microcapsules and pure hexylacetate microcapsules (no catalyst). Finally self-healing samples were composed of epoxy resin, E-glass reinforcement, HOPDMS/PDES microcapsules and DBTL/hexylacetate microcapsules. Control 2 samples were designed to mimic the mechanical behavior of self-healing samples, but without the ability to polymerize the healing agents.

2.3. Sample preparation

All composite panels (275 mm × 95 mm) were manufactured with Epon 862/Epikure W (Miller-Stephenson), at a mix ratio of

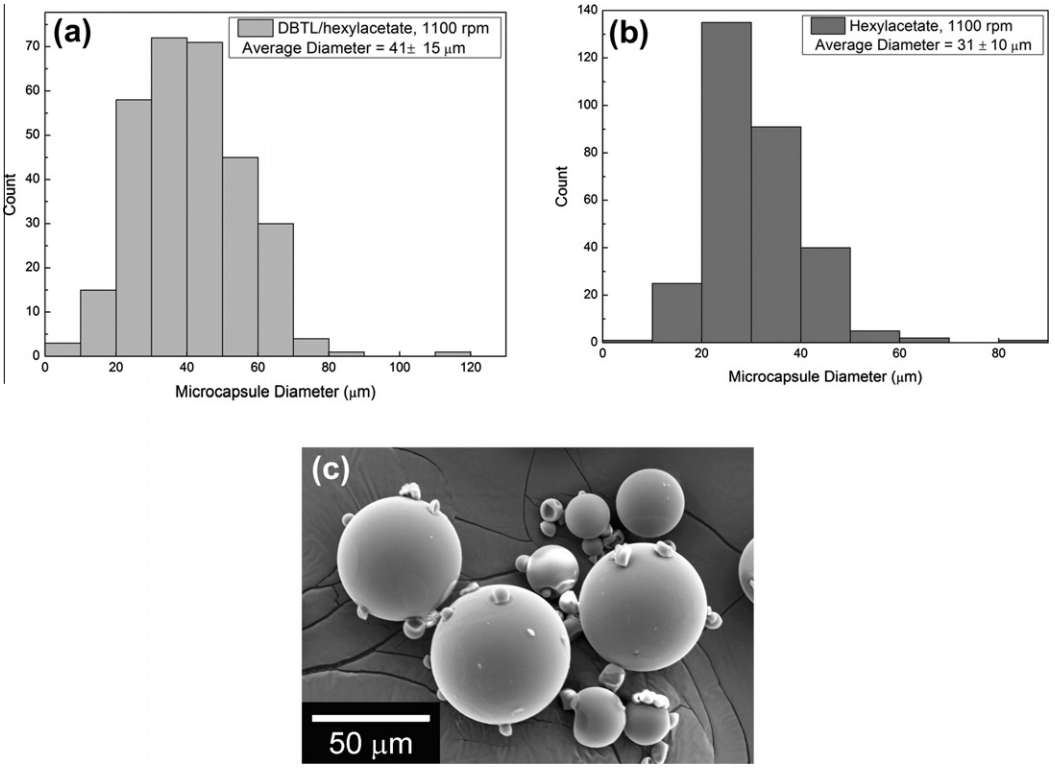

Fig. 2. Summary of DBTL/hexylacetate and hexylacetate microcapsules used in the healing portion of this study: (a) DBTL/hexylacetate microcapsules prepared at an agitation rate of 1100 rpm with a number average diameter of 41 μm, (b) hexylacetate microcapsules prepared at an agitation rate of 1100 rpm with an number average diameter of 31 μm, (c) Scanning electron microscope image of 41 μm DBTL/hexylacetate capsules.

Table 1
Summary of sample types and components.

Component	Control 1	Control 2	Self-healing
Epoxy resin	Epon 862/Epikure W	Epon 862/Epikure W	Epon 862/Epikure W
Reinforcement	8H satin weave E-glass	8H satin weave E-glass	8H satin weave E-glass
Type A capsules	–	HOPDMS/PDES 25 μm or 42 μm	HOPDMS/PDES 25 μm or 42 μm
Type B capsules	–	Hexylacetate 31 μm	DBTL/hexylacetate 41 μm

100:26.4, epoxy resin and an eight harness satin weave E-glass (Style 7781, Fiber Glast) reinforcement. The microcapsules were mixed (10:1 by weight, HOPDMS/PDES:DBTL/hexylacetate or hexylacetate) into the unreacted epoxy resin followed by 30 min of degassing at 100 °C. A wet layup procedure was used with the plies sequenced $(0,90,0)_s$, where 0 represents the warp direction. A schematic of the layup procedure is shown in Fig. 3. A Teflon plate was placed underneath to create a smooth surface finish from which the sample could be easily removed. The composite sample was laid up layer by layer with liquid epoxy resin wetting out each ply. Stringent control of composite thickness and fiber volume fraction was critical for accurate comparison of sealing results between different specimens, for this reason a non-standard manufacturing method was used. The composite thickness (1.92–2.03 mm) was regulated by steel spacers placed around the periphery and a porous steel plate was placed on top allowing resin to flow through into bleeder cloths above. As pressure was applied, the sample compacted until the porous plate came into contact with the steel spacers, thus dictating the sample thickness and fiber volume fraction (0.35). The entire layup was cured under 170 kPa at 121 °C for 8 h.

Fig. 4 shows a polished cross section of a control 2 sample with 42 μm average diameter HOPDMS/PDES microcapsules. The composite is free of voids and the microcapsules are evenly distributed

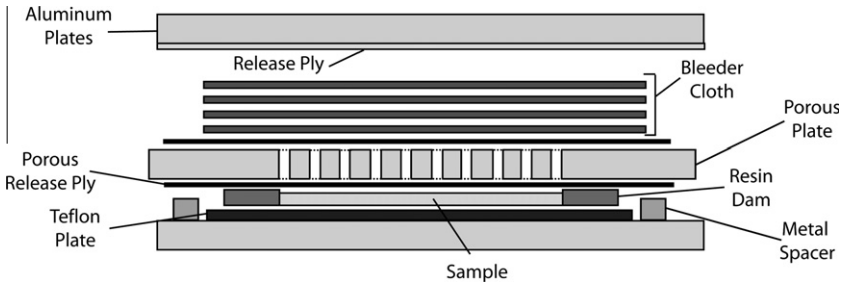

Fig. 3. Schematic of composite sample layup components.

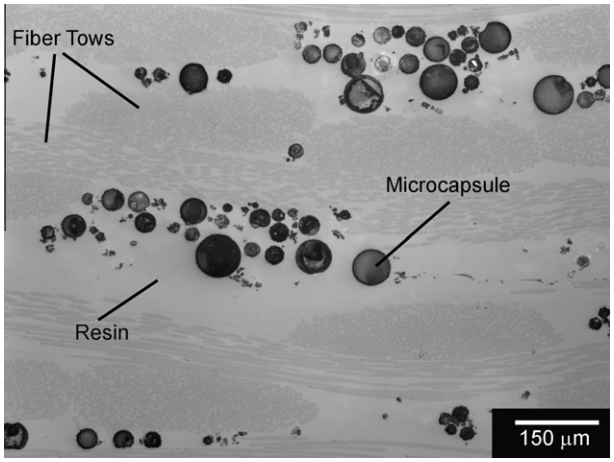

Fig. 4. Cross-sectional image of an undamaged region of a control 2 composite sample with 42 μm average diameter HOPDMS/PDES and 31 μm hexylacetate microcapsules.

in the matrix rich regions between the fiber tows running both parallel and perpendicular to the plane of the image. The microcapsule concentrations were calculated based on polished cross-sectional micrographs such as these.

2.4. Mechanical testing

Composite panels were sectioned into smaller 45 mm × 45 mm samples. Mechanical damage was introduced by cyclically driving an indenter tip into the sample 10 times per side to a maximum load of 690 N. The complete details of this damage protocol are outlined in Moll et al. [8]. Fig. 5 shows a tiled cross-sectional optical image of a control 2 sample containing 11 vol.% 25 μm capsules after the damage protocol showing a large crack spanning the entire thickness of the sample.

After damage was induced, samples were allowed to heal for approximately 12 h before leak testing. Healed samples were placed in a pressure cell apparatus [8] and pressurized nitrogen gas (276 kPa) was applied to one side of the sample while monitoring the pressure on the opposite side for 30 min. A sample was considered fully healed if the output pressure did not increase by more than 70 Pa over the entire test. A minimum of six specimens were used to evaluate sealing performance for each sample type.

Short beam shear experiments were performed, according to ASTM standard D2344 [12], on samples approximately 4 mm wide × 25 mm long. Prior to testing, the samples were conditioned for at least 48 h at 23 °C and 50% relative humidity. Samples were loaded in 3-point bending at a rate of 1 mm/min with an 8 mm span between bottom supports. The load and displacement data were recorded and short beam strength, F^{sbs}, was calculated from:

$$F^{sbs} = 0.75 \times \frac{P_m}{b \times h} \quad (1)$$

where P_m is the peak load, b is the sample width, and h is the thickness.

Dynamic mechanical analysis (DMA) was also performed on samples, eight weeks after manufacturing, to obtain the storage modulus and T_g following ASTM standard D5023-07 [13]. After conditioning at 23 °C and 50% relative humidity for a minimum of 48 h, the samples were loaded into a DMA (TA Instrument RSA III) in 3-point bending with a span of 25 mm. The temperature of the sample was ramped from 20 °C to 160 °C at a rate of 3 °C/min. The storage and loss moduli were recorded as a function of temperature. The glass transition temperature (T_g) is reported as the peak in the tangent of the phase angle curve.

3. Results

3.1. Sealing performance

The effect of microcapsule size and concentration on self-healing performance was investigated for number average microcapsule diameters of 25 μm and 42 μm. Fig. 6 compares the healing performance of various microcapsule concentrations and sizes to that of the control samples. Although control 1 samples do not have the ability to heal, 14% of the samples did not leak due to insufficient damage. Self-healing samples with 8 vol.% 25 μm microcapsules sealed 75% of the time, compared to control 2 samples that sealed only 29% of the time. We hypothesize that the small percentage of control 2 samples that sealed in this case may be due to the presence of the viscous HOPDMS liquid in the crack network. Increasing both the size and the concentration of microcapsules (9 vol.% 42 μm and 11 vol.% 25 μm microcapsules), resulted in 100% sealing compared to 0% for the representative control 2 samples. The delivery of more healing agents by increasing capsule size and/or concentration improves healing performance. The decrease in sealing performance for control 2 samples is due to the increased microcracking associated with these samples, as was previously shown by Moll et al. [8].

3.2. Effect of microcapsule concentration on mechanical properties

The effect of microcapsule concentration on the short beam strength (SBS), storage modulus and T_g were investigated for composite samples with 0–15 vol.% microcapsules. Representative SBS loading curves for all microcapsule (15 μm HOPDMS and 23 μm DBTL/hexylacetate capsules at a ratio of 10:1) concentrations tested are plotted in Fig. 7. All samples failed in shear. We found that the short beam strength decreased as the concentration of capsules in the composite increased, as summarized in Fig. 8. Samples without any microcapsules present (control 1) had a short beam strength of 57 MPa. A small decrease in SBS occurred for composites with 6 wt.% and 9 wt.% microcapsules. When the

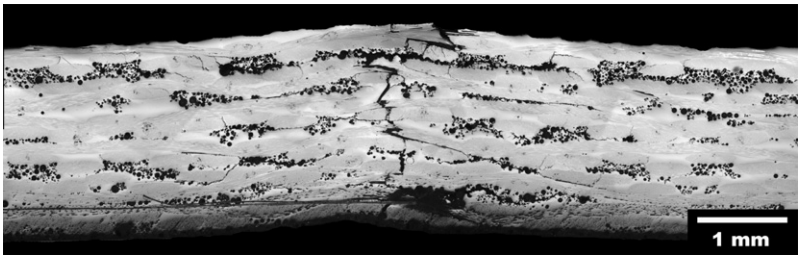

Fig. 5. Cross-sectional image of a control 2 sample with 11 vol.% 25 μm HOPDMS/PDES capsules after damage showing a large crack running from one side of the sample to the other.

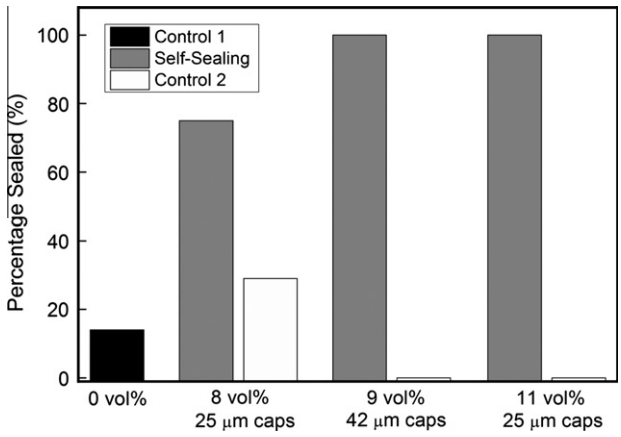

Fig. 6. Effect of microcapsule size and concentration on sealing performance for self-healing composites.

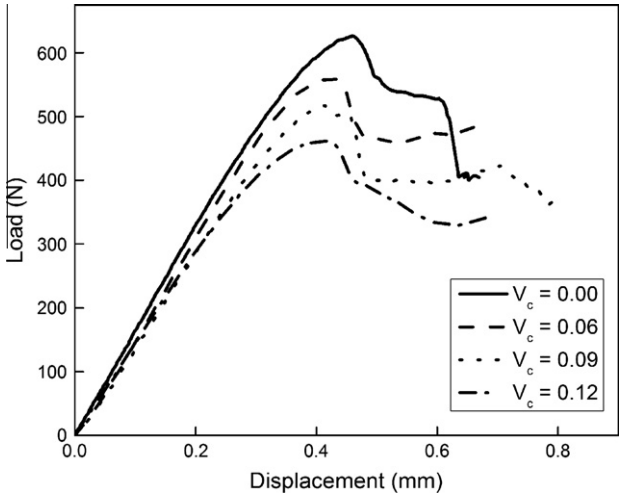

Fig. 7. Representative short beam shear loading curves for composite samples with varying microcapsule concentrations. V_c is capsule volume fraction in the composite.

amount of capsules was increased further to 12 vol.%, the SBS decreased by nearly 30%. Much has been reported in literature about the effect of the addition of particulates on the interlaminar shear strength (ILSS) of continuous fiber reinforced composites. For micron scale particulates, Yuan et al. described an initial increase in ILSS with the addition (2–5 wt.%) of 86–200 μm microcapsules in a glass fiber reinforced epoxy composite, but upon further increasing the particulate concentration the ILSS decreased [14]. Sainathan et al. reported a decrease in ILSS of glass fiber reinforced epoxy laminates with the addition of 2–4 wt.% 20 μm graphite particles [15]. The addition of nanoscale core shell rubber particles to carbon fiber/epoxy [16] and nanoclay to glass fiber/diallyl phthalate composites [17] both increased the interlaminar shear strength. Interestingly, recent work by Jin [18] reports improved dispersion and only a 14% drop in SBS with identical capsules, loaded at ca. 12 vol.% (7.5 wt.%) in a different epoxy resin (Araldite/Aradur 8605). Based on this data, we speculate that the SBS performance of microcapsule filled composites can be improved by judicious selection of the resin and process conditions, as well as better control of capsule size and bonding characteristics.

The storage modulus at 25 °C was measured for microcapsule (25 μm HOPDMS and 31 μm pure hexylacetate capsules at a ratio of 10:1) concentrations ranging from 0 to 15 vol.% (Fig. 9). The

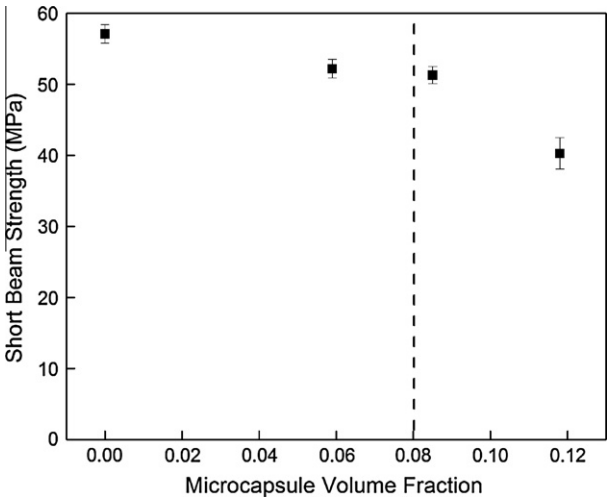

Fig. 8. Composite short beam strength as a function of microcapsule concentration. Vertical line represents the minimum microcapsule concentration used for healing in this study. Error bars represent one standard deviation.

storage modulus decreased by 15% with the addition of 15 vol.% microcapsules. Experimental values were compared with the model developed by Naik and Shembekar [19–22] for satin weave composites in Fig. 9. The matrix properties were modified by reducing the matrix stiffness proportionally to the concentration of capsules, assuming the capsules did not contribute to the stiffness. A rule of mixtures relationship was used. The model over predicts the composite modulus at higher concentrations of microcapsules indicating that the microcapsules may disrupt the woven fiber architecture, reducing the overall stiffness of the composite.

The T_g of fiber-reinforced composites and non-reinforced epoxy resin samples was also measured for varying microcapsule concentrations (25 μm HOPDMS and 31 μm pure hexylacetate capsules at a ratio of 10:1) as seen in Fig. 10. As the microcapsule concentration increased, the T_g decreased slightly for both the neat resin and the composite. To determine if the decrease in T_g was caused by the capsule components leaching out of the microcapsules and plasticizing the matrix, we prepared additional samples of epoxy with 0.55 wt.% HOPDMS. The amount of HOPDMS mixed

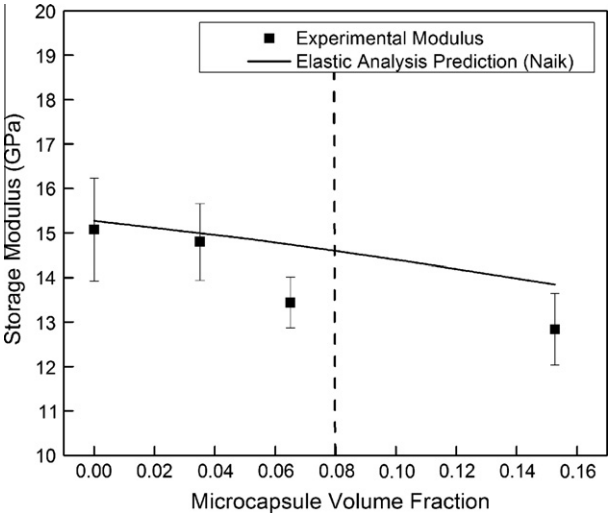

Fig. 9. Effect of microcapsule concentration on composite storage modulus. Vertical line represents the minimum microcapsule concentration used for healing in this study. Error bars represent one standard deviation.

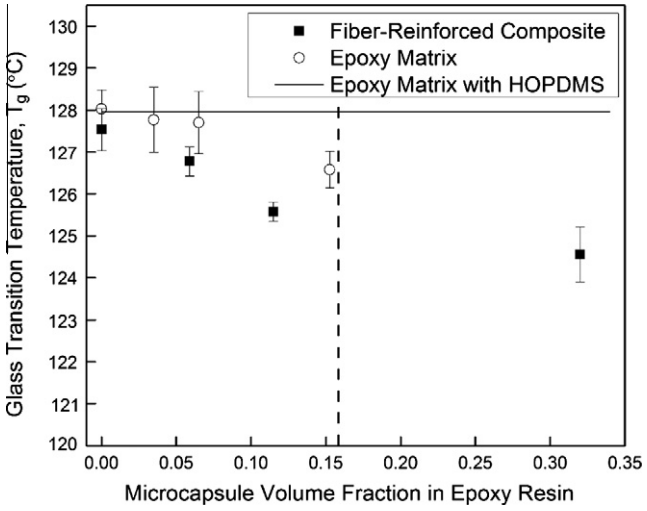

Fig. 10. Glass transition temperature as a function of microcapsule concentration in fiber reinforced composites and epoxy samples. Microcapsule volume fractions are reported in the resin only, not accounting for the inclusion of fiber reinforcement. Horizontal line represents the T_g of epoxy resin combined with 0.55 wt.% HOPMDS monomer. Vertical line represents the minimum microcapsule concentration used for healing in this study. Error bars represent one standard deviation.

directly into the resin was equivalent to volume of healing agent that would be released if 14% of the microcapsules ruptured in epoxy resin with a capsule loading of 5 vol.% (a much higher concentration than we would expect as a result of capsule damage during processing). No drop in T_g was observed with the addition of HOPDMS. Similar trends have been reported for the addition of particulates in composites by Crowson and Arridge [23], who showed a decrease in the T_g of a glass bead reinforced epoxy resin with increasing bead concentration. Also, Yuan et al. [14] found that in a glass fiber reinforced epoxy composite with epoxy resin filled microcapsules the T_g of the composite decreased with increasing microcapsule concentration.

4. Conclusions

A fully cured, moderate glass transition temperature (127 °C) E-glass reinforced self-healing composite with self-sealing functionality was achieved by the incorporation of a thermally stable healing chemistry comprised of hydroxyl end-functionalized polydimethylsiloxane (HOPDMS) and cross-linking agent polydiethoxysiloxane (PDES) catalyzed by dibutyltin dilaurate (DBTL). Encapsulated healing components (25–42 μm average diameter) were incorporated into the matrix rich regions of the sample during fabrication. This is the first demonstration of microcapsule based autonomic self-healing in a fully cured, moderate T_g material. Previously, only 67% of composite samples with a low T_g matrix, were capable of self-healing [8]. The current PDMS based healing chemistry has achieved sealing in 100% of fully cured T_g composite samples when 9 vol.% 42 μm capsules or 11 vol.% 25 μm capsules are dispersed in the matrix. The effect of microcapsule concentration on short beam strength, and storage modulus were investigated for composite samples with capsule concentrations from 0 to 15 vol.%. At a concentration of 12 vol.%, a 30% decrease in the short beam strength and at 15 vol.% a 15% reduction in storage modulus were measured. The glass transition temperature (T_g) of the fiber-reinforced composite and plain epoxy resin was also reduced slightly, ca. 3 °C, with the addition of 15 vol.% microcapsules.

Acknowledgement

The authors gratefully acknowledge funding provided by NASA (Contract #NNL10AA07C).

References

[1] Bechel VT, Negilski M, James J. Limiting the permeability of composites for cryogenic applications. Compos Sci Technol 2006;66(13):2284–95.
[2] Choi HS, Jang YH. Bondline strength evaluation of cocure/precured honeycomb sandwich structures under aircraft hygro and repair environments. Compos Part A – Appl Sci Manuf 2010;41(9):1138–47.
[3] Yokozeki T, Ogasawara T, Aoki T, Ishikawa T. Experimental evaluation of gas permeability through damaged composite laminates for cryogenic tank. Compos Sci Technol 2009;69(9):1334–40.
[4] Choi S, Sankar BV. Gas permeability of various graphite/epoxy composite laminates for cryogenic storage systems. Compos Part B – Eng 2008;39(5):782–91.
[5] McVay AC, Johnson WS. Permeability of various hybrid composites subjected to extreme thermal cycling and low-velocity impacts. J Compos Mater 2010;44(12):1517–31.
[6] Beiermann BA, Keller MW, Sottos NR. Self-healing flexible laminates for resealing of puncture damage. Smart Mater Struct 2009;18(8).
[7] Kalista SJ. Self-healing of poly(ethylene-co-methacrylic acid) copolymers following projectile puncture. Mech Adv Mater Struct 2007;14(5):391–7.
[8] Moll JL, White SR, Sottos NR. A self-sealing fiber-reinforced composite. J Compos Mater 2010;44(22):2573–85.
[9] Mangun CL, Mader AC, Sottos NR, White SR. Self-healing of a high temperature cured epoxy using poly(dimethylsiloxane) chemistry. Polymer 2010;51(18):4063–8.
[10] Cho SH, Andersson HM, White SR, Sottos NR, Braun PV. Polydimethylsiloxane-based self-healing materials. Adv Mater 2006;18(8):997–1000.
[11] Cho SH, White SR, Braun PV. Self-healing polymer coatings. Adv Mater 2009;21(6):645–9.
[12] ASTM-D2344. Standard test method for short-beam strength of polymer matrix composite materials and their laminates; 2006.
[13] ASTM-D5023-07. Standard test method for plastics: dynamic mechanical properties. In: Flexure (three-point bending); 2006.
[14] Yuan L, Gu A, Lian G, Wu J, Wang W, Sun Z. Novel glass fiber-reinforced cyanate ester/microcapsule composites. J Compos Mater 2009;43(16):1679–94.
[15] Sainathan N, Padmanabhan K, Sashidhara S, Rao RMVGK, Kishore. Influence of particulate graphite additions on the shear related behavior of glass fabric reinforced epoxy composites. J Reinf Plast Compos 1995;14(5):445–57.
[16] Day RJ, Lovell PA, Wazzan AA. Toughened carbon/epoxy composites made by using core/shell particles. Compos Sci Technol 2001;61(1):41–56.
[17] Kong ZX, Wang JH. Interlaminar shear strength of glass fiber reinforced dially phthalate laminates enhanced with nanoclays. Adv Mater Res 2009;79–82:1779–82.
[18] Jin H. Self-healing of high temperature cured epoxy and composites. University of Illinois at Urbana-Champaign, Aerospace Engineering; 2012.
[19] Naik NK, Shembekar PS. Elastic behavior of woven fabric composites 3. Laminate design. J Compos Mater 1992;26(17):2522–41.
[20] Naik NK, Ganesh VK. Prediction of on-axes elastic properties of plain weave fabric composites. Compos Sci Technol 1992;45(2):135–52.
[21] Naik NK, Shembekar PS. Elastic analysis of woven fabric laminates 2. Mixed composites. J Compos Technol Res 1993;15(1):34–7.
[22] Naik N. Woven fabric composites. Lancaster, Pennsylvania: Technomic Publishing Company, Inc.; 1994.
[23] Crowson RJ, Arridge RGC. Elastic properties in bulk and shear of a glass bead reinforced epoxy-resin composite. J Mater Sci 1977;12(11):2154–64.